ACKNOWLEDGMENTS

We wish to thank the staff of the Tandem Van de Graaff at Florida State University and the plate counters under the direction of Mary Jones and also the operating staff of the Los Alamos Omega West Reactor. Helpful critical discussions were held with Dr. Authur Kerman and Dr. M. E. Bunker. The assistance of Dr. E. T. Jurney, Parvin Lippincott and Mrs. K. H. Harper is gratefully acknowledged. We are especially indebted to Dr. O. W. B. Schult and his coworkers for allowing us to quote the low-energy capture data prior to its publication.

PHYSICAL REVIEW VOLUME 136, NUMBER 2B 26 OCTOBER 1964

Decay of Xe^{137} †

RONALD J. ONEGA* AND WILLIAM W. PRATT
Department of Physics, The Pennsylvania State University, University Park, Pennsylvania
(Received 10 June 1964)

The decay of Xe^{137} was studied by means of scintillation techniques. The radioactive samples were produced by means of neutron irradiation of natural xenon, which contains 8.87% Xe^{136}. The half-life of Xe^{137} was found to be 3.95±0.11 min. One gamma ray of 0.455±0.003 MeV was attributed to Xe^{137}. An upper limit of 0.03 of the intensity of this gamma ray is placed on any other gamma ray due to the decay of Xe^{137}. The end-point energy of the beta spectrum was found to be 4.06±0.06 MeV using K^{42} as a calibration check. A beta ray was found to be in coincidence with the 0.46-MeV gamma ray. A Kurie plot of the beta-gamma coincidence spectrum as well as a subtraction method of the singles Kurie plot were both in agreement with 3.60±0.06 MeV for the lower-energy beta group. In order to get the intensity of the two beta transitions, two independent methods were utilized. These indicated a relative intensity of about 0.33±0.03 for the 3.60-MeV beta-ray group and 0.67±0.03 for the 4.06-MeV beta-ray group. Log*ft* values indicate first-forbidden beta-ray selection rules for both transitions. This is found to be in accord with shell-model predictions. A decay scheme is proposed on the basis of these results.

I. INTRODUCTION

THE beta-ray spectrum associated with the 3.9-min activity of Xe^{137} has previously been studied by absorption techniques.[1,2] Energies of 4 MeV[1] and 3.5 MeV[2] were reported. The gamma-ray spectrum has been investigated using scintillation techniques.[3,4] A gamma ray of 0.44 MeV was reported which decayed with a half-life of about four minutes and which was attributed to the decay of Xe^{137}. The work reported here was undertaken in order to obtain a more definitive study of the beta-ray spectrum, to search for additional gamma rays, and to relate the decay scheme of Xe^{137} to the energy level structure of Cs^{137}.

II. EXPERIMENTAL PROCEDURE

In the present investigation sources were prepared by irradiating natural xenon gas in the Pennsylvania State University Research Reactor. The procedure for handling the gas from the shipping container was as follows: Displace about half of the water in a 50-ml polyethylene bottle with xenon gas; expose the sample of gas in the reactor; transfer the irradiated gas from the polyethylene exposure bottle to a counting cell. The counting cell was an aluminum cylinder with a polyethylene window approximately 1 mil thick.

Beta- and gamma-ray spectra were studied using conventional methods of scintillation spectroscopy. A 3-×3-in. NaI(Tl) crystal was used for measuring the gamma-ray spectra and was also used in conjunction with a 2-×2-in. NaI(Tl) crystal for coincidence measurements. A 2-×2-in. anthracene crystal was used for the beta-ray measurements. Beta-gamma coincidence measurements employed the 3-in. NaI(Tl) crystal and

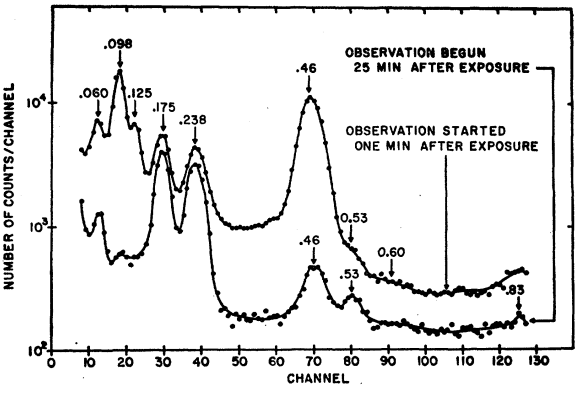

FIG. 1. Xe^{137} gamma-ray spectrum for energies less than 0.85 MeV; observations 24 min apart.

† This work was supported in part by the U. S. Atomic Energy Commission.
* Present address: Department of Physics, Virginia Polytechnic Institute, Blacksburg, Virginia.
[1] H. Born and W. Seelmann-Eggebert, Naturwiss. **31**, 201 (1943).
[2] S. Nassiff and W. Seelmann-Eggebert, Z. Naturforsch. **10a**, 83 (1955).
[3] S. Prakash, Z. Elektrochem. **64**, 1037 (1960).
[4] D. W. Ockenden and R. H. Tomlinson, Can. J. Chem. **40**, 1594 (1962).

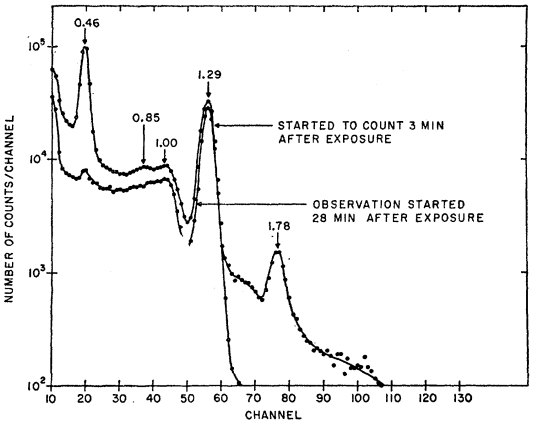

FIG. 2. High-energy gamma-ray spectrum for Xe^{137}; observations 25 min apart.

the 2-in. anthracene crystal. The instrumentation included a 128-channel pulse-height analyzer and a fast-slow coincidence circuit with a resolving time (τ) of 0.25 μsec.

III. GAMMA-RAY MEASUREMENTS

The gamma-ray spectra were obtained with the 3-in. NaI(Tl) crystal shielded by a lead collimator. Figure 1 shows a typical spectrum in the energy range less than 0.85 MeV. The gas had been transferred from the exposure bottle so that no gamma rays detected could be due to activity induced in the polyethylene exposure bottle. The upper curve is a plot of the spectrum which was obtained by starting the observation one minute after exposure and counting for 13.1 min. Gamma rays of 0.06, 0.10, 0.18, 0.24, 0.46, 0.53, possibly 0.60, and 0.83 MeV can be observed. The 0.06-MeV peak is thought to be a composite peak of 0.05 and 0.07 MeV which has been observed in other spectra.

The lower curve of Fig. 1 was obtained using the same sample and the same geometry, the count beginning 25 min after irradiation. There is some indication that the 0.60-MeV gamma ray is still present, as are the 0.06, 0.18, 0.24, 0.46, 0.53, and 0.83 MeV gamma rays. The only gamma ray that decays with a half-life comparable to that measured by Sugarmann[5] (3.9 min) is the 0.46 MeV gamma ray. The half-life obtained for this gamma ray, which is the average of seven measurements, is 3.98±0.12 min. The error is the root-mean-square deviation of the seven values from the average.

All other gamma-ray peaks, except for the 0.83-MeV peak, can be accounted for by the decay of other xenon isotopes. The 0.83-MeV photopeak is attributed to Mg^{27} (see below).

The upper spectrum shown in Fig. 2 was obtained by starting the observation 3 min after exposure. Gamma rays of 0.46, 0.85, 1.00, 1.29, and 1.78 MeV are observed. The lower curve shows the spectrum obtained 25 min later. The 1.29-MeV peak is obviously due to an isotope with a much longer half-life than 4 min; the half-life indicates it to be due to an Ar^{41} activity. The 1.78-MeV gamma ray has completely disappeared; half-life measurements indicate that this peak is due to Al^{28}. Table I summarizes the data obtained by gamma-ray measurements.

Although the presence of aluminum in the system is not understood, we are unable to account in any other way for the gamma rays of 1.78 MeV [$Al^{27}(n,\gamma)Al^{28}$], 1.00 MeV [$Al^{27}(n,p)Mg^{27}$], and 0.85 MeV [$Al^{27}(n,p)Mg^{27}$]. Both the energy and half-life of the 1.78-MeV gamma ray are clearly characteristic of Al^{28}. Although the 1.00- and 0.85-MeV gamma rays are weak, and both energy and half-life measurements are difficult, an extensive study of these (including source exposures at the reactor core and behind a thermal column with a reduced ratio of fast to slow neutrons) indicates that they are most probably due to the (n,p) reaction on Al^{27}.

Twenty spectra were obtained with the 0.46-MeV gamma-ray peak. The average value of the energies of the photopeaks corresponding to the 0.46-MeV gamma ray was 0.455±0.003 MeV.

The error quoted here represents the standard deviation of the twenty individual determinations from the average result, and is thus indicative of random errors only. Any systematic errors of which we are aware are estimated to be negligible. A similar statement applies to errors quoted below in connection with determinations of half-lives, beta-ray end-point determinations, and relative intensities.

Gamma-gamma coincidence measurements were attempted by searching for gamma rays in coincidence with the 0.455-MeV gamma ray. All such measurements gave negative results.

TABLE I. Summary of gamma-ray data.

Gamma-ray observed (MeV)	Observed half-life	Proposed source	Accepted energy (MeV)	Accepted half-life
0.05	>1 h	$Xe^{124}(n,\gamma)Xe^{125}$	0.0547	18 h
0.07	>1 h	$Xe^{124}(n,\gamma)Xe^{125}$	0.0746	18 h
0.11	1.0 min	$Xe^{124}(n,\gamma)Xe^{125m}$	0.112	55 sec
0.14	1.0 min	$Xe^{126}(n,\gamma)Xe^{127m}$	0.125	75 sec
0.19	15 h	$Xe^{124}(n,\gamma)Xe^{125}$	0.1876	18 h
0.24	15 h	$Xe^{124}(n,\gamma)Xe^{125}$	0.2425	18 h
0.35[a]	...	$Xe^{134}(n,\gamma)Xe^{135}$	0.36	9.1 h
0.455	3.95 min	$Xe^{136}(n,\gamma)Xe^{137}$	0.46	3.9 min
0.46[a]	...	$Xe^{124}(n,\gamma)Xe^{125}$	0.46	18 h
0.53	~30 min	$Xe^{134}(n,\gamma)Xe^{135m}$	0.53	16 min
0.60[a]	...	$Xe^{134}(n,\gamma)Xe^{135}$	0.604	9.1 h
0.84	5.5 min	$Al^{27}(n,p)Mg^{27}$	0.834	9.5 min
1.00	~5.5 min	$Al^{27}(n,p)Mg^{27}$	1.015	9.5 min
1.28	>1 h	$Ar^{40}(n,\gamma)Ar^{41}$	1.29	1.83 h
1.77	2.5 min	$Al^{27}(n,\gamma)Ar^{28}$	1.78	2.3 min

[a] Gamma-ray intensity too low to obtain a lower limit on the half-life.

[5] N. Sugarmann, J. Chem. Phys. **17**, 11 (1949).

IV. THE BETA-RAY SPECTRUM

Half-Life

Xe^{125}, Xe^{127}, Xe^{135}, and Ar^{41} isotopes contribute to the gamma spectrum (see Table I) so that the beta spectrum is expected to contain these contaminants also. However, the highest energy beta group that arises from any of these isotopes is 1.5-MeV (Ar^{41} has a very weak 2.49-MeV beta group whose influence is expected to be negligible). The decay rate of the high-energy region of the beta spectrum will thus be unaffected by these contaminants although the region below 1.5 MeV will contain long lived components.

Figure 3 shows the different decay rates of the lower and upper parts of the beta spectrum. The upper curve was taken about five minutes later than the lower curve and the higher energy regions of the spectra were normalized to each other. The half-life of the beta spectrum was determined by observing the decay of the high-energy region. Five determinations of the Xe^{137} half-life were made. A half-life of 3.82 ± 0.23 min was determined.

Calibration

The internal conversion peaks of Cs^{137} and Bi^{207} and the end-point energy of the K^{42} beta spectrum were used to calibrate the apparatus. By using the two internal conversion points of 0.63 and 0.97 MeV, a straight line was drawn giving the energy as a function of channel number in the 128-channel analyzer.

Since these two internal conversion electron peaks are both less than 1 MeV and the beta-ray end-point energy of Xe^{137} is in the neighborhood of 4 MeV, an extreme extrapolation of the calibration curve is necessary. K^{42} was used as a calibration check because of the range of this extrapolation. The end-point energy of K^{42}, which has been obtained by means of a thin lens spectrometer,[6] is given as 3.545 ± 0.010 MeV. A Kurie plot for K^{42} was made using the calibration curve obtained from the Cs^{137} and Bi^{207} internal conversion points. If the end-point energy of K^{42} obtained in this manner came within 0.10 MeV of the 3.545-MeV value, then a calibration point corresponding to the K^{42} end-point energy so determined was inserted on the calibration curve, i.e., the calibration curve was not altered. If, on the other hand, the K^{42} end-point energy was outside of this 0.10-MeV limit, the calibration curve was adjusted to give agreement within this limit. Having obtained in this manner a calibration curve with a known error at the K^{42} end-point energy, a value for the Xe^{137} end-point energy was determined. This value was then corrected by an amount corresponding to the known error obtained for the K^{42} end-point energy.

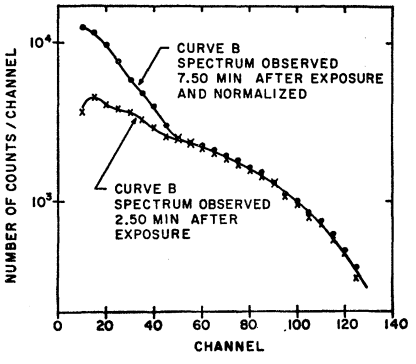

FIG. 3. Beta spectrum of xenon showing different rates of decay between the high-and low-energy regions.

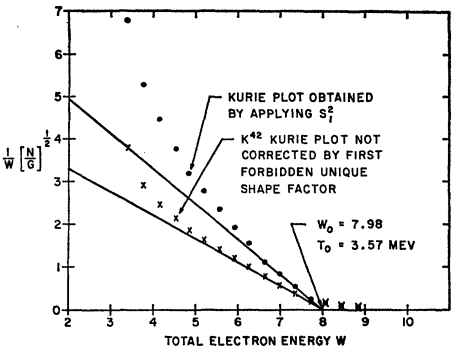

FIG. 4. The corrected Kurie plot of K^{42} using the corrected calibration.

The 3.55-MeV beta group of K^{42} is of the first forbidden unique type so that a correction factor $S_1^2(W)$[7] must be applied to make its shape resemble an allowed or a nonunique first forbidden transition. Figure 4 shows the effect of this correction factor. The resulting deterioration in the shape of the Kurie plot is a consequence of instrumental distortion.

Thirteen Kurie plots of the beta spectrum were made for Xe^{137}, and the end-point energy was determined to be 4.04 ± 0.07 MeV.

Our method of calibrating the beta-ray spectrometer, which basically involves a comparison of the Xe^{137} end-point energy with the well-known K^{42} end-point energy, succeeds, we believe, in largely eliminating any systematic errors other than those associated with the fitting of a straight line to the points on the Kurie plot. In view of the relatively small region of linearity of the Kurie plot obtained with our scintillation spectrometer, and also of the presence of two beta-ray groups relatively close together in energy, the fitting of this straight line necessarily requires some subjective judgment which may involve appreciable and unknown errors. We believe that the best measure of these errors, which will appear in both energy and relative intensity determinations, will be manifest in the degree of con-

[6] A. V. Pohm, R. C. Waddell, and E. N. Jensen, Phys. Rev. **101**, 1315 (1956).

[7] E. Konopinski, in *Beta and Gamma Ray Spectroscopy*, edited by K. Siegbahn (North-Holland Publishing Company, Amsterdam, The Netherlands, 1955).

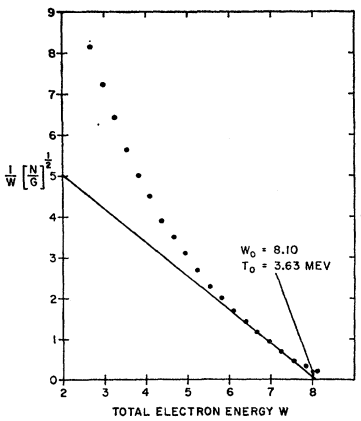

FIG. 5. Xe^{137} beta-gamma coincidence spectrum Kurie plot.

sistency of the data, i.e., in the extent to which several independent determinations agree with each other. Accordingly, we assign errors to the beta-ray end-point energy determinations, as well as to the relative intensity determinations described below, which are based on the standard deviations of several independent measurements from the average result.

Beta-Gamma Coincidence Measurements

The 3-in. crystal was used as a gamma detector for beta-gamma coincidence measurements. A single-channel analyzer window was adjusted to accept pulses corresponding to the 0.46-MeV gamma ray, the output from this analyzer then being used to gate the multichannel analyzer in which the beta spectrum was recorded. A Kurie plot of the coincidence beta spectrum was made in the same manner as for the singles spectrum. Figure 5 is an example of such a Kurie plot. The result of eleven independent coincidence measurements gives a beta-ray end-point energy of 3.65±0.10 MeV.

The beta-gamma coincidence measurements show that the 0.46-MeV gamma ray is in coincidence with a 3.65-MeV beta transition. The total energy difference between the Xe^{137} ground state and the ground state of Cs^{137} determined from these values is found to be 4.11±0.10 MeV, which is to be compared with the value of 4.04±0.07 MeV obtained from the measurement of the singles beta spectrum.

A weighted average of these two determinations of the total transition energy, the weights being taken inversely proportional to the square of the errors, is 4.06±0.06 MeV. This would indicate a best value of 3.60±0.06 MeV for the lower beta transition energy.

The Lower Energy Beta Group

The beta spectrum of Xe^{137} is complex. The beta-gamma coincidence Kurie plot should be due to only one beta group. That two beta groups exist in the singles spectrum is suggested by the extent of the straight line portion of the coincidence Kurie plot compared with that of the singles Kurie plot. The lengths of the straight line portions of these Kurie plots are 0.30 and 0.18 of their total energy ranges, respectively. A subtraction procedure was attempted in order to obtain, by a separate method, the end-point energy of the inner beta group and to obtain its relative intensity. The subtraction procedure consisted of the following steps:

(i) Extrapolate the straight line portion of the singles Kurie plot back to zero kinetic energy.

(ii) Using this straight line, compute the number of counts in each energy interval that correspond to the high-energy beta group.

(iii) Subtract the number of counts so obtained from the original number of counts used in the computation of the Kurie plot.

(iv) Using this difference, calculate another Kurie plot, now having the higher energy beta rays subtracted.

(v) Extrapolate the straight line portion of this Kurie plot to the energy axis to obtain the end-point energy of the inner beta group.

Figure 6 shows the original Kurie plot and the Kurie plot obtained by means of the subtraction procedure; in this case the end-point energy of the inner beta group was 3.55 MeV. This subtraction procedure was performed on seven of the singles spectra to yield an energy of 3.56±0.13 MeV. It will be recognized that, due to the very limited straight line regions of the Kurie plots, this subtraction procedure will not be expected to be very accurate. Nevertheless, the close agreement between the end-point energy determined in this way and that obtained in the coincidence measurements tends to lend confidence to the conclusion that the beta spectrum has two components separated in energy by the energy of the one observed gamma ray.

V. THE BETA DECAY BRANCHING RATIO

The relative intensity of the two beta-ray groups must be known in order to determine logft values and thus obtain an indication of the beta decay transition selection rules. Three methods were used to obtain the branching ratio. The first method makes use of the Kurie plots which were computed in the subtraction

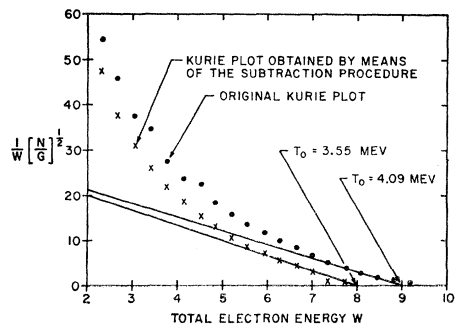

FIG. 6. Subtraction technique yielding the lower energy beta group of Xe^{137}.

procedure to obtain the energy of the inner beta group. The other two methods employ comparison techniques, comparing measurements on Xe^{137} with similar measurements on Ar^{41}.

Kurie Plot Method

The subtraction technique used in obtaining the lower energy beta spectrum necessitates the computation of $N_1(W)$, the number of counts due to those beta transitions that lead to the ground state of Cs^{137} with energy W; from this is obtained a second Kurie plot representing the lower energy beta group. Integrating $N_1(W)$ over energy yields the total number of transitions that populate the ground state of Cs^{137}.

$N_2(W)$, the number of counts due to beta rays that populate the excited state of Cs^{137}, was obtained by extrapolating the short straight line portion of the second Kurie plot back to zero kinetic energy thus eliminating instrumental distortion of the spectrum. The number of counts corresponding to the points along this line was computed and is $N_2(W)$. $N_2(W)$ was integrated over the energy range available to it. The total number of transitions populating the excited state of Cs^{137} was thus obtained.

The branching ratio obtained in this way is found to be 0.55 ± 0.14; this value being the result of seven separate measurements. This corresponds to $35\%\pm6\%$ of the β rays populating the first excited state.

Comparison Method

Ar^{41} decays into K^{41} by means of two beta groups. The higher energy beta group of 2.49 MeV leads to the ground state of K^{41} and the lower energy beta group of 1.20 MeV populates the first excited state. The quantity $f_2(\mathrm{Ar})$, the fraction of the beta rays from argon populating the excited state of K^{41}, is 0.991 and the fraction $f_1(\mathrm{Ar})$ of the beta rays leading to the ground state is 0.009.[8] Only one γ ray, of 1.29 MeV, results following the decay of Ar^{41}. The Ar^{41} and Xe^{137} decay schemes are thus similar, both having two beta groups and one gamma ray.

The first comparison method involves a determination of the ratio of beta-gamma coincidences to beta singles. The ratio of the beta-gamma coincidence to beta ray single counting rate for argon is

$$N_{\beta-\gamma}(\mathrm{Ar})/N_\beta(\mathrm{Ar})=f_2(\mathrm{Ar})\omega_\gamma(\mathrm{Ar})\epsilon_\gamma(\mathrm{Ar})R(\mathrm{Ar}),$$

where $N_{\beta-\gamma}(\mathrm{Ar})$ = beta-gamma coincidence counting rate for argon, $N_\beta(\mathrm{Ar})$ = beta-ray counting rate for argon, $f_2(\mathrm{Ar})$ = the fraction of the beta rays leading to the excited state in K^{41}, $\omega_\gamma(\mathrm{Ar})$ = solid angle subtended by the argon source to the 3-×3-in. NaI(Tl) crystal, $\epsilon_\gamma(\mathrm{Ar})$ = the gamma-ray efficiency for the argon γ ray, $R(\mathrm{Ar})$ = the ratio of the area of the 1.29-MeV peak covered by the single-channel analyzer window to the total peak area. By using an identical experimental arrangement for the Xe^{137} case, the ratio of the beta-gamma coincidence to beta-ray single counting rate is

$$N_{\beta-\gamma}(\mathrm{Xe})/N_\beta(\mathrm{Xe})=f_2(\mathrm{Xe})\omega_\gamma(\mathrm{Xe})\epsilon_\gamma(\mathrm{Xe})R(\mathrm{Xe}).$$

These symbols have the same meaning as above except for applying to the xenon case.

The solid angles are identical and can be eliminated, yielding

$$f_2(\mathrm{Xe})=f_2(\mathrm{Ar})\frac{N_{\beta-\gamma}(\mathrm{Xe})/N_\beta(\mathrm{Xe})}{N_{\beta-\gamma}(\mathrm{Ar})/N_\beta(\mathrm{Ar})}\frac{\epsilon_\gamma(\mathrm{Ar})R(\mathrm{Ar})}{\epsilon_\gamma(\mathrm{Xe})R(\mathrm{Xe})}.$$

All quantities on the right side of this equation are known. The ratio of the gamma-ray efficiencies is obtained from the computation of the total absolute efficiency and from the ratio of the peak area to total area for the two gamma rays.[9] The ratio of the efficiencies of the Ar^{41} to Xe^{137} gamma rays was found to be 0.36.

Data were obtained for six determinations of $f_2(\mathrm{Xe})$ by this method. The average result obtained from these measurements of f_2 was $32\%\pm4\%$. No corrections were made for the effects of anisotropy in the beta-gamma angular correlation. The two counters (with 90° between their axes) were both placed close to the source so that large solid angles were subtended, thus tending to attenuate drastically any angular correlations. An estimate of the maximum effect expected, based on measurements of beta-gamma cascades with similar spin sequences, indicates any anisotropy effect to be an order of magnitude less than the error quoted in the result.

The second comparison method utilizes the ratio of the gamma-ray counting rate to the beta-ray counting rate. The expression for $f_2(\mathrm{Xe})$ using this method is

$$f_2(\mathrm{Xe})=\frac{N_\gamma(\mathrm{Xe})/N_\beta(\mathrm{Xe})}{N_\gamma(\mathrm{Ar})/N_\beta(\mathrm{Ar})}f_2(\mathrm{Ar})\frac{\epsilon_\gamma(\mathrm{Ar})}{\epsilon_\gamma(\mathrm{Xe})}\frac{R(\mathrm{Ar})}{R(\mathrm{Xe})}\frac{\epsilon_\beta(\mathrm{Xe})}{\epsilon_\beta(\mathrm{Ar})},$$

where the last factor is the ratio of the beta-ray counter efficiencies for xenon and argon. $N_\gamma(\mathrm{Xe})$ is the gamma-ray counting rate from xenon, $N_\gamma(\mathrm{Ar})$ is the argon gamma-ray counting rate. The last factor is assumed to be equal to one. The quantity $f_2(\mathrm{Xe})$ was computed using this equation and yields a value of $30\%\pm12\%$ for the fraction of the beta rays that populate the first excited state of Cs^{137}.

The average value of the three determinations of $f_2(\mathrm{Xe})$, weighted by the reciprocal of their errors squared, yields $33\%\pm3\%$ for the value of $f_2(\mathrm{Xe})$.

VI. RESULTS AND SUMMARY

The half-life obtained from the gamma-ray spectra was 3.98 ± 0.12 min, whereas the beta-ray data yield a

[8] A. Schwarzschild, B. M. Rustad, and C. S. Wu, Phys. Rev. **103**, 1796 (1956).

[9] R. L. Heath, in Scintillation Spectrometry Gamma Spectrum Phillips Petroleum Company, Atomic Energy Division, Idaho Falls, Idaho, 1 July 1957, Appendixes I and II (unpublished).

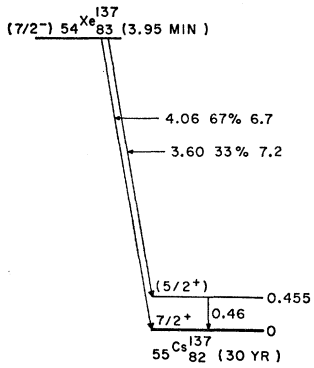

FIG. 7. Proposed decay scheme of Xe^{137}.

half-life of 3.82±0.23 min. A weighted average of these results in a half-life of 3.95±0.11 min for the decay of Xe^{137}.

All of the observed contaminants in the gamma-ray spectra are due to various isotopes of xenon with the exception of Ar^{40} and Al^{27}. Some of these contaminants are ascribed to isomeric transitions in Xe^{125}, Xe^{127}, and Xe^{135}. All of the gamma-ray peaks can be accounted for with some certainty, the only one due to Xe^{137} being a gamma ray of 0.455±0.003 MeV.

Two beta groups were found. The upper level in Cs^{137} is populated by 33%±3% of the transitions and the ground state is populated by 67%±3% of the transitions. The energies of these two groups are 3.60±0.06 and 4.06±0.06 MeV, respectively. From these data, the logft values of the two transitions can be obtained. The logft value for the ground-state transition is 6.7 and for the first-excited-state transition it is 7.2. These values fall most probably in the category of first forbidden nonunique transitions.

The foregoing data indicate the decay scheme shown in Fig. 7. The ground-state spin and the magnetic moment of Cs^{137} have been obtained by atomic beam methods,[10] giving a spin and parity of $\frac{7}{2}+$. From the logft value and the shell model, the ground-state spin and parity of Xe^{137} can be assigned to be $\frac{7}{2}-$. The spin and parity of the first excited state of Cs^{137} is indicated to be $\frac{5}{2}+$ from the shell model and logft value for the lower energy beta transition.

ACKNOWLEDGMENTS

We wish to thank the staff of the Research Reactor, and especially Douglas S. Vonada, for their generous and unfailing assistance with all of the measurements involved in this work.

[10] *Nuclear Data Sheets* (Printing and Publishing Office, National Research Council—National Academy of Sciences, Washington 25, D. C.).

PHYSICAL REVIEW VOLUME 136, NUMBER 2B 26 OCTOBER 1964

Study of the 7.285-MeV Level in Lead-208 Using a Rotor Technique

B. ARAD, G. BEN-DAVID, AND Y. SCHLESINGER
Israel Atomic Energy Commission, Soreq Research Establishment, Yavne, Israel
(Received 9 June 1964)

The 7.285-MeV level in Pb^{208}, excited by thermal neutron capture gamma rays from iron, was studied using a rotating target to vary the energy of the gamma rays seen by the target. Energy shifts of −1.07, −1.75, +1.65, and +2.57 eV were achieved, and the observed changes in scattered intensity are consistent with the resonant Pb^{208} level lying 6.5±1 eV below the iron capture gamma-ray line.

INTRODUCTION

RESONANT scattering of gamma rays has recently been reported[1–5] using the high-energy gamma rays emitted by various nuclei in the capture of thermal neutrons. These scattering events occur when the energy of the capture gamma-ray line (corrected for target recoil) happens to lie close to a suitable resonance level in the target nucleus. Figure 1 shows schematically the Doppler broadened emission line and resonant level, with an energy separation of δ eV between the two maxima. The effective scattering cross section $\sigma_{\gamma\gamma}$ is given by the energy integral of the product of these two curves and hence is very sensitive to the value of δ. As the Doppler widths of these lines are usually of the

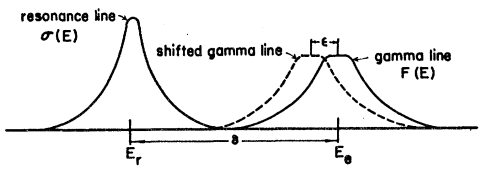

FIG. 1. Schematic representation of the resonance level and the capture gamma emission line. The dashed curve shows the shift produced by rotation of the target.

[1] G. Ben-David (Davis) and B. Huebschmann, Phys. Letters **3**, 87 (1962).
[2] C. S. Young and D. J. Donahue, Phys. Rev. **132**, 1724 (1963).
[3] H. H. Fleischmann and F. W. Stanek, Z. Physik **175**, 172 (1963).
[4] B. Arad (Huebschmann), G. Ben-David (Davis), I. Pelah, and Y. Schlesinger, Phys. Rev. **133**, B684 (1964).
[5] B. Arad, G. Ben-David, I. Pelah, and Y. Schlesinger, International Conference on Nuclear Physics with Reactor Neutrons, Argonne, October 15–17, 1963, ANL-6797 (unpublished).